



NMR Imaging of the honeybee brain

Authors: Haddad, D., Schaupp, F., Brandtm, R., Manz, G., Menzel, R., et al.

Source: Journal of Insect Science, 4(7) : 1-7

Published By: Entomological Society of America

URL: <https://doi.org/10.1673/031.004.0701>



NMR Imaging of the honeybee brain

D. Haddad¹, F. Schaupp², R. Brandt², G. Manz², R. Menzel², A. Haase¹

¹Physikalisches Institut EP5, Universität Würzburg, Germany

²Institut für Biologie - Neurobiologie, Freie Universität Berlin, Germany

dhaddad@physik.uni-uerzburg.de

Received 11 August 2003, Accepted 18 January 2004, Published 12 March 2004

Abstract

NMR microscopy provides non-invasively distinct soft-tissue contrast in small biological samples. We were able to visualize the three-dimensional structure of the honeybee brain in its natural shape in the intact head capsule. Thus, in addition to acquiring detailed information about the shapes and volumes of the different brain compartments, we were able to show their relative orientations toward each other within the head capsule. Since the brain was lightly fixed but not dehydrated, and stayed attached to the head capsule and its internal structures, the NMR experiments exhibited larger volumes and a more natural stereo geometry of the various brain structures compared to confocal laser microscopy experiments on dissected, dehydrated and cleared brains.

Keywords: *Apis mellifera carnica*, nuclear magnetic resonance

Abbreviation:

CLM confocal laser microscopy

NMR nuclear magnetic resonance

Introduction

Three-dimensional ¹H Nuclear Magnetic Resonance (NMR) microscopy is a powerful tool for investigating the inner structure of small biological objects without surgical procedures. Combined with their distinct soft-tissue contrast, NMR methods provide excellent conditions for non-invasive tissue characterization and phenotyping of small animals.

Honeybees are an important model in neurobiology. This is due to their rather simply structured nervous system and their striking cognitive capabilities (Menzel and Giurfa 2001). For example, their ability to communicate information about the location and quality of a new feeding place via their dance (Frisch 1965), shows that they possess important mechanisms for rapid neural processing, establishing a stable memory and subsequently communicating the memorized information (Menzel and Müller 1996). Thus, in neurobiology honeybees are a common model system for analyzing underlying neural mechanisms. Furthermore, by investigating the bee brain's anatomy, correlations between anatomy and function can be studied. Since the 19th century, the anatomy of the honeybee's brain has been studied by dissecting the brain from the head capsule (Dujardin 1850). Unfortunately, the bee brain's three-dimensional structure and stereo geometry is altered by this handling and the subsequent fixation of the brain outside the head capsule. Therefore, until recently the establishment of a standard bee brain model had to be based on data from deformed

dissected brains (Brandt et al. in preparation). A detailed description of the bee brain's gross and fine anatomy can be found in (Mobbs 1985).

We performed NMR microscopy experiments on formalin-fixed honeybee samples to visualize in great detail the anatomy of the honeybee brain still in place in the intact head capsule (external and internal cuticular structures). Thanks to the non-invasive character of the NMR experiments, deformations due to the dissection of the brain from the head capsule could be avoided here, revealing the brain's true natural shape. Due to the high spatial resolution, even small compartments of the brain are clearly visible in the NMR images. Thus, with NMR it was possible to analyze the natural three-dimensional shape and geometry of the various brain structures and substructures (Figure 1). Therefore, NMR microscopy allows us to establish a standard bee brain model of the brain in its natural shape inside and relative to the head capsule.

Materials and Methods

Sample preparation

The heads of eight *Apis mellifera carnica* foraging workers, were cut from the thoraxes and fixed with a 4% formalin/ 0.1% Triton X solution while evacuating them lightly for 30 minutes. After keeping the heads in 4% formalin solution over night at approximately 4° C, they were rinsed with iso-osmotic sucrose solution (450 mOsm/l) for 2 hours and subsequently stored in 30%

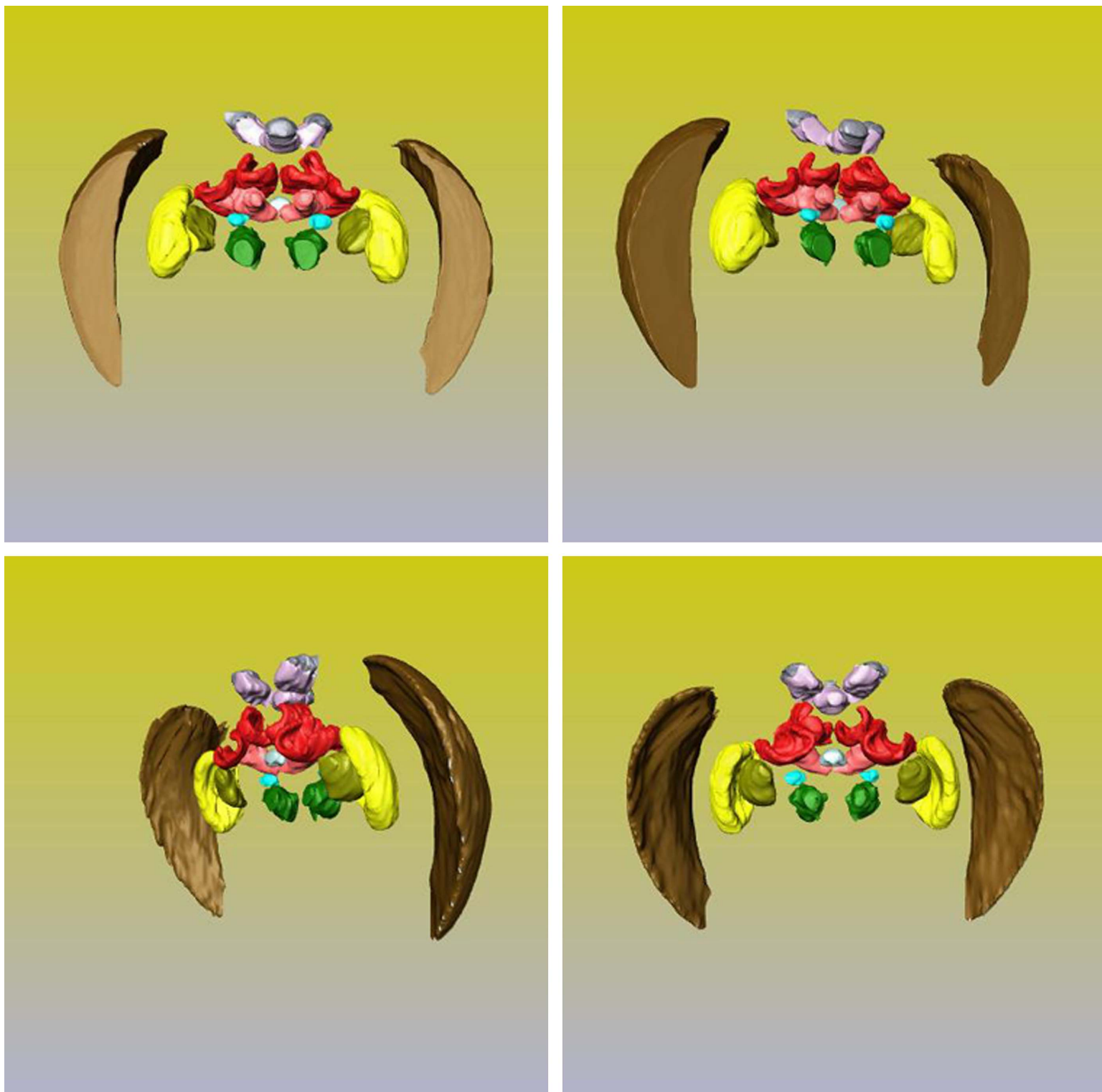


Figure 1. Different orientations of 3D surface reconstructions from a manually- segmented 3D dataset with a nominal resolution of $15.6 \times 15.6 \times 30.0 \mu\text{m}^3$. The segmented brain structures are the optic lobes of *Apis mellifera* with medulla and lobula (yellow), the antennal lobes (green), the peduncles and β -lobes (light red), the α -lobes (light red), the paired calyces (red), the lateral ocelli (pink), median ocellar tract (grey), optic tubercles (light blue) and the compound eyes (brown). The different angles under which the surface reconstructions are shown provide a good impression of bee brain's stereo geometry.

ethanol. In order to remove dissolved gases, the ethanol was evacuated for 10 minutes beforehand. Prior to the NMR experiments the ethanol was replaced with iso-osmotic sucrose solution to increase the signal-to-noise-ratio (Bossart et al. 1999) and to avoid swelling

or shrinking the brains. The heads were evacuated again for 10 minutes to remove dissolved gases and to exchange the ethanol. The mandibles had to be removed to fit the bee heads into the NMR tubes that had an inner diameter of 3.6 mm.

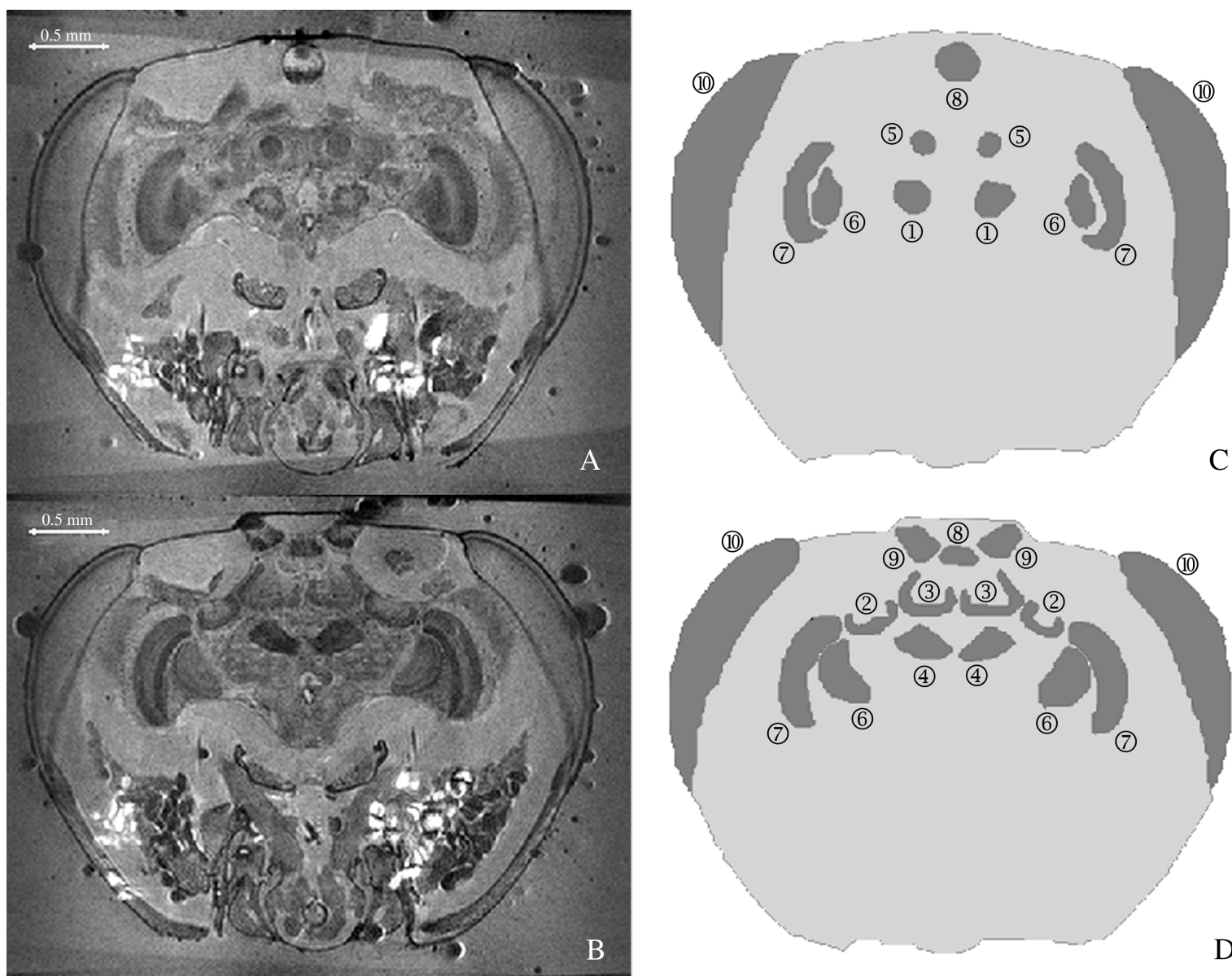


Figure 2. a) and b) NMR images of the *Apis mellifera* brain. Both images are slices of a three-dimensional dataset with a nominal resolution of $15.6 \times 15.6 \times 30.0 \mu\text{m}^3$. Slice b) is located posterior to slice a). Images c) and d) show the corresponding segmentation masks, all manually segmented structures are shown in dark grey. The brain structures visible in the images are: antennal lobe (1, green in Figure 1), lateral (2, red) and median (3, red) calyx, peduncle and β -lobe (4, light red), α -lobe (5, light red), lobula (6, yellow), medulla (7, yellow). The other marked structures are the median (8, grey) and lateral (9, pink) ocelli and the compound eyes (10, brown).

NMR hardware

A specially-designed NMR probehead with a solenoid coil was used for the proton NMR experiments. The coil had a length of 5.5 mm and an inner diameter of 4.0 mm. All measurements were performed at 11.75 T on a Bruker AMX500 spectrometer with a maximum gradient strength of 0.66 T/m. During the experiments, a constant coil and sample temperature of 5°C was maintained.

NMR experiments

Two-dimensional (2D) Spin Echo images were acquired with a nominal inplane resolution (before zero filling) of $15.6 \times 15.6 \mu\text{m}^2$ and a slice thickness of $100 \mu\text{m}$, in order to position a coronal slice through the brain. The field of view (FOV) was $4.0 \times 4.0 \text{ mm}^2$, using a 256×256 matrix. Subsequently, three-dimensional (3D) spin echo images with up to $256 \times 256 \times 60$ voxels were acquired (FOV $4.0 \times 4.0 \times 0.9 \text{ mm}^3$) to obtain images of the whole brain with nominal resolutions of up to $15.6 \times 15.6 \times 30.0 \mu\text{m}^3$. For the 2D and 3D experiments echo times (T_E) ranging from 8.2 to 25.0 ms and repetition times (T_R) ranging from 1.0 to 1.5 s were used, leading to a total experiment time of less than 26 hours for a 3D experiment with 4 averages. Even this small number of averages sufficed to provide a signal-to-noise-ratio in the images which was high enough for manual segmentation of the different brain structures. Zero filling by a factor of 2 in each dimension was performed during the data processing, leading to image resolutions of up to $7.8 \times 7.8 \times 15.0 \mu\text{m}^3$.

Two-dimensional (2D) Spin Echo images were acquired with a nominal inplane resolution (before zero filling) of $15.6 \times 15.6 \mu\text{m}^2$ and a slice thickness of $100 \mu\text{m}$, in order to position a coronal slice through the brain. The field of view (FOV) was $4.0 \times 4.0 \text{ mm}^2$, using a 256×256 matrix. Subsequently, three-dimensional (3D) spin echo images with up to $256 \times 256 \times 60$ voxels were acquired (FOV $4.0 \times 4.0 \times 0.9 \text{ mm}^3$) to obtain images of the whole brain with nominal resolutions of up to $15.6 \times 15.6 \times 30.0 \mu\text{m}^3$. For the 2D and 3D experiments echo times (T_E) ranging from 8.2 to 25.0 ms and repetition times (T_R) ranging from 1.0 to 1.5 s were used, leading to a total experiment time of less than 26 hours for a 3D experiment with 4 averages. Even this small number of averages sufficed to provide a signal-to-noise-ratio in the images which was high enough for manual segmentation of the different brain structures. Zero filling by a factor of 2 in each dimension was performed during the data processing, leading to image resolutions of up to $7.8 \times 7.8 \times 15.0 \mu\text{m}^3$.

Surface reconstructions

For one three-dimensional dataset the different compartments of the honeybee brain were manually segmented and reconstructed to polygonal surface models. Direct volume rendering of the 3D datasets and surface and volume calculations from the segmented structures were also performed. This post-processing of the NMR images was performed with the Amira graphics software package (ZIB, Berlin; Indeed Visual Concepts GbmH, Berlin; TGS; <http://www.amiravis.com>).

Results

NMR microscopy images

The detailed anatomy of the honeybee brain is well-represented in the NMR images (Figure 2) and video (see the videos at <http://insectscience.org/4.7>). The achieved nominal spatial resolution of up to $15.6 \times 15.6 \times 30.0 \mu\text{m}^3$ was sufficient to visualize the anatomy of the brain with the main neuropils (e.g. optic lobes, antennal lobes, mushroom bodies) and several of their substructures.

As the brain was left in the head capsule, deformations due to dissecting the brain out of the head capsule do not occur. Only a small shrinkage of less than 5% due to the initial formalin fixation is to be expected. During several weeks in which the NMR experiments were performed repeatedly with the same samples, no changes in the anatomy of the samples or the structure of the tissue could be observed in the NMR images, nor did the image contrast change.

As can be easily seen in the NMR images, the honeybee's brain is stretched out in the head capsule between the compound eyes on both sides with the antennal nerves in the front, and the ocelli in the upper part of the head and the connectives to the subesophageal ganglion in the back.

The two optic lobes are clearly visible in the NMR images.



Figure 3. The arrows indicate the ray-like connections (lamina) between the optic lobes (medullas) and the compound eyes of *Apis mellifera*. The image is a slice from a 3D NMR dataset and has a nominal resolution of $15.6 \times 15.6 \times 30.0 \mu\text{m}^3$.

They process the visual information gathered by the compound eyes and are located laterally at both sides of the brain (Figure 1, yellow structures). The three ganglia of each optic lobe, the lamina, medulla and lobula, are well separated in the NMR images, as are their respective subcompartments (ommatidia in the compound eyes, columns in lamina and medulla, strata in the lobula (Figure 2 # 7, 6). Bundles of axons of the retinula cells in the compound eye projecting to the lamina are also well-resolved (see Figure 3).

The glomeruli forming the antennal lobes (Figure 1, green structures), the primary olfactory neuropil, can just barely be resolved in the NMR images (see Figure 2 # 1). These substructures are small spherical units with diameters of $15 - 30 \mu\text{m}$ (Galizia et al. 1999). Therefore, the larger glomeruli are detectable, but not the smaller ones, because their diameters are too close to the resolution limit of the NMR images.

Both optical and antennal lobes are connected to the calyx region of the mushroom bodies. The mushroom bodies are large structures in the center of the bee brain, consisting of the paired calyces (Figure 1, dark red structures), α -lobes and β -lobes and the peduncles (see Figure 1 light red structures). In the NMR images the dense packing and parallel arrangement of intrinsic neuron axons in the lower part of the mushroom bodies appear as very dark structures (Figure 2 # 4, 5). In particular, the extremely dense peduncles are among the darkest structures in the images. The paired calyces are located at the dorsal end of the mushroom bodies (Figure 1, dark red structures). Although with their thickness of only $30-40 \mu\text{m}$ they are relatively small, they are clearly visible in the NMR images (Figure 2 # 2, 3). The mushroom bodies are known to be involved in complex brain functions such as learning, memory and social behavior (Menzel et al. 1988). The volumes of the whole mushroom bodies and their compartments change with age and experience (Durst et al. 1994; Withers et al. 1993), indicating that behavioral plasticity is reflected by structural plasticity.

The three ocelli on the dorsal midline area are visible (Figure 2 # 8, 9; see also Figure 1, grey and pink structures). Their function is not well understood, but might be related to overall light adaptation, horizon detection and fast control of flight behavior using illumination contrast in large visual fields (Kastberger 1990).

Furthermore, with NMR microscopy, not only is the brain visualized, but also other compartments in the head, the compound eyes (Figure 2 # 10) and various internal and external head cuticular structures (e.g. the tentorium, which separates the brain from the mandible region). Several glands, especially mandibular glands, can also be seen in the NMR images, as well as different muscles (not shown in the images here).

Surface reconstruction and volume rendering

In order to gain a better impression of the three-dimensional geometry of the honeybee brain in the head capsule, three-dimensional polygonal surface models of the different brain structures and a direct volume rendering of one whole 3D NMR dataset were performed. Prior to calculating the surface reconstruction shown in Figure 1, it was necessary to perform a manual segmentation of the different brain structures in the NMR images. Manual segmentation in this context describes the process of manually assigning individual image points to specific structures of the bee brain, thus creating a new dataset which represents a

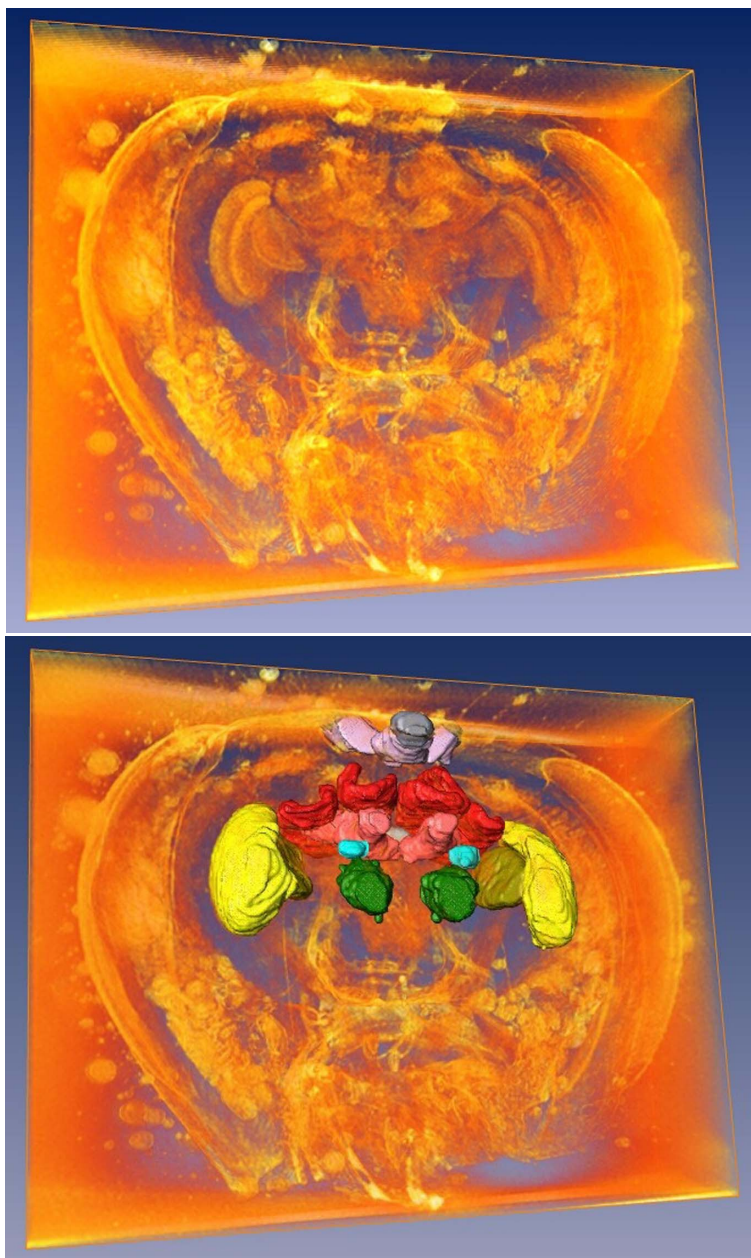


Figure 4. Volume rendering of a 3D dataset (top) with overlaid 3D surface reconstruction (bottom) of the *Apis mellifera* brain. The semi-transparent image provides a good three-dimensional impression of the brain's stereo geometry and with the overlaid surface reconstructions shows the relative orientation of brain structures in relation to the bee's head capsule. Further-more, fine boundaries, e.g. between the different parts of the medulla are shown very distinctly.

mask of the different structures seen in the NMR images.

The direct volume rendering of the NMR dataset is shown in Figure 4 (left image). The semi-transparent way of displaying the image data allows us to visualize the 3D shape and stereo geometry of the whole brain in one image, thus showing the position of the different brain structures in the bee's head, their relative orientations and possible paths for neural connections.

In the right image of Figure 4 the surface reconstructions are superimposed onto the volume rendering of the same three-

dimensional dataset. Although the solid structures hide some of the tissue behind them, this superposition puts more emphasis on the segmented brain structures and provides a more detailed impression of their shapes and locations within the bee's head capsule. Furthermore, this image provides an estimation of the relative sizes of the different brain structures. Additional insight in the stereo geometry of the brain structures can be obtained from movie sequences of the NMR images and rotating surface reconstructions (see the videos at <http://insectscience.org/4.7>).

Volume calculations

Volume calculations were performed using the manually segmented brain structures. The arithmetic mean values of both hemispheres of the brain are listed in Table 1. In the calculations the relative error for the single structures in each hemisphere was estimated in the range of $\pm 10\%$. This estimation was based on two effects: First, the intrinsic error of the NMR experiments resulting from gradient imperfections and partial volume effects, and secondly, the fact that the segmentation was performed manually.

The intrinsic error of the NMR experiments was measured using a calibration phantom with glass tubes of different known diameters and proved to be less than $\pm 4\%$.

In order to quantify the error resulting from the manual segmentation, the NMR data were analyzed by two independent observers to evaluate the inter-observer differences, and a medium sized structure (right antennal lobe) was segmented 22 times by the same observer to determine the intra-observer differences. Since each individual error was less than $\pm 2.5\%$, the maximum combined error for the manual segmentation was about $\pm 5\%$.

Not surprisingly, in comparison with images from confocal laser microscopy (CLM) (Brandt et al. 2004 in preparation), the NMR images exhibit larger volumes for most of the different brain structures, because the optical measures were performed with dehydrated and cleared brains (Table 1). Only the densely packed lower parts of the mushroom bodies show smaller values. Depending on the single structure, the volumes measured with NMR were larger by a factor of 1.05 - 1.30 than the volumes measured with CLM (Table 1). The median of the comparison for the enlarged structures was a factor of 1.23.

In our opinion these results correlate well to the fact that the honeybee's brain is stretched out in the head capsule between its attachment points, e.g. the compound eyes, the antennae and the ocelli. The larger volumes obtained from the NMR experiments

Table 1. Comparison of *Apis mellifera* brain structure volumes calculated from 3D surface reconstructions of segmented NMR and CLM datasets.

Neuropil	Volume NMR	Volume CLM	Ratio
	[$10^7 \mu\text{m}^3$]	[$10^7 \mu\text{m}^3$]	NMR / CLM
medulla	5.99 ± 0.42	5.73 ± 0.62	1.05
lobula	1.95 ± 0.14	1.65 ± 0.14	1.18
antennal lobe	1.40 ± 0.10	1.08 ± 0.15	1.29
median calyx	1.52 ± 0.11	1.24 ± 0.13	1.23
lateral calyx	1.76 ± 0.13	1.35 ± 0.14	1.30
mushroom bodies w/o calyces	1.30 ± 0.09	1.58 ± 0.15	0.82

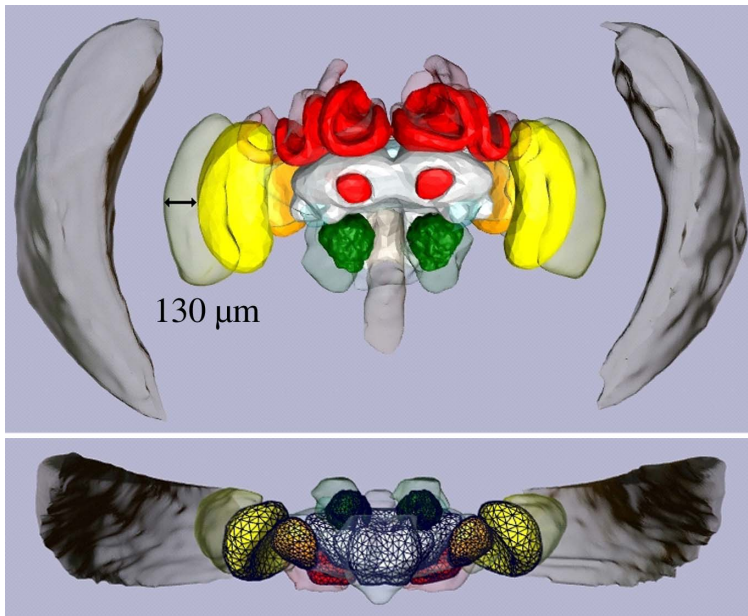


Figure 5. Surface reconstructions of segmented datasets from NMR (shaded) and CLM (solid) measurements of *Apis mellifera* brains. The large displacements of the different brain structures are obvious.

reflect, not only the tension under which the brain tissue is held in the head capsule, but also the reduced shrinkage of the brain when it is fixed in the still intact head capsule instead of being dissected from the head capsule and subsequently fixed, dehydrated and cleared outside the head capsule. Inter-individual volume differences may also contribute to the different results from NMR and CLM measurements. However, since CLM images from 19 adult honeybee workers of the same beehive only showed differences in the brain size of the individuals that were so small that they could be neglected against the error due to the manual segmentation of the data, we conclude that the larger volumes measured with NMR microscopy predominantly reflect the lack of histological artifacts and are thus much closer to the in vivo situation.

In addition to the overall volume differences, the stereo geometry of the brain is altered during the dissection from the head capsule and the histological procedures applied for CLM imaging, as shown in Figure 5, where surface reconstructions of segmented brain structures from CLM and NMR experiments are compared. The images show that the structures of dissected brains are positioned much closer to each other and are no longer spread out as they were before, due to the tension from being attached inside the head capsule.

The medullae and lobulae, for instance, are tilted further outwards in the NMR images for more than half their thickness. Especially the lower ends are located much closer to the corresponding compound eyes. The antennal lobes are located closer to the front of the bee's head and the calyces stand further upright than in the CLM images. Thus, the deformation of the brain during the dissection is not negligible. Absolute values for the displacements of the different structures are difficult to interpret, since, for example, the linear displacement of 130 μm for the left medulla measured in Figure 5a is the cumulative result of the displacement

of the medulla and of the structures closer to the center of the bee brain.

Discussion

Here the three-dimensional structure of the honeybee brain has to our knowledge been studied for the first time very close to its natural shape in the intact head capsule. Thanks to the non-invasiveness of the NMR experiments, the brain was still stretched out between its attachment points in the head capsule, and merely needed to be lightly fixed and neither dehydrated nor cleared. Thus, we were not only able to obtain detailed information about the shapes and volumes of the different brain compartments, but also to determine their relative orientations toward each other in the surrounding head capsule. Compared to CLM experiments, the brain in the NMR images is tilted outward, which again correlates well to the fact that the brain is stretched out and kept under tension in the head capsule. Based on the results from NMR microscopy it is now possible to establish a standard bee brain model of the brain close to its natural shape in the head capsule. The existing results from other imaging techniques of dissected brains can be implemented in this new standard model of the brain in its natural shape by using nonaffine correction algorithms to morph the obtained dissected geometry to the natural geometry in the head capsule (Rohlfing et al. 2001, 2003).

In conclusion, the NMR microscopy experiments allow visualizing the honeybee brain in its natural shape that, combined with the existing CLM data, allow us to quantify the small but significant changes in the size and stereo geometry of the different brain structures that take place during the dissection and subsequent fixation of the brain outside the head capsule.

References

- Bossart EL, Inglis BA, Silver XS, and Mareci TH. 1999. The Effect of Fixative Solutions in Magnetic Resonance Imaging. *Proceedings 7th ISMRM Conference*, Philadelphia.
- Brandt R, Rohlfing T, Steege A, Zöckler M and Menzel R. in preparation. A three-dimensional average-shape atlas of the honeybee brain based on confocal images of 20 subjects.
- Dujardin F. 1850. Mémoire sur le système nerveux des insectes. *Annales des Sciences Naturelles Zoologie* B14: 195-206.
- Durst C, Eichmüller S, Menzel R. 1994. Development and experience lead to increased volume of subcompartments of the honeybee mushroom body. *Behavioral and Neural Biology* 62: 259-263.
- von Frisch K. 1965. *Tanzsprache und Orientierung der Bienen*. Heidelberg: Springer
- Galizia CG, McIlwraith SL, Menzel R. 1999. A digital 3D atlas of the honeybee antennal lobe based on optical sections acquired using confocal microscopy. *Cell and Tissue Research* 295: 383-394.
- Kastberger G. 1990. The ocelli control the flight course in honeybees. *Physiological Entomology* 15: 337-346.
- Menzel R, Giurfa M. 2001. Cognitive architecture of a mini-brain: the honeybee. *Trends in Cognitive Sciences* 5, no. 2: 62-71.

- Menzel R, Michelsen B, Ruffer P, Sugawa M. 1988. Neuropharmacology of learning and memory in honeybees. In: Herting G, Spatz HC editors. *Synaptic transmission and plasticity in nervous systems*. Berlin: Springer.
- Menzel R, Müller U. 1996. Learning and memory in honeybees: From behavior to neural substrates. *Annual Review of Neuroscience* 19: 379-404.
- Mobbs PG. 1985. Brain structure. In: Kerkut GA, Gilbert LI editors. *Comprehensive insect physiology biochemistry and pharmacology*. 1st edition. Oxford: Pergamon Press.
- Rohlfing T, Brandt R, Maurer CR, Menzel R. 2001. Bee Brains, B-Splines and computational democracy: generating an average shape atlas. *Proceedings of the IEEE Workshop on Mathematical Methods in Biomedical Image Analysis*, MMBIA, Kauai, Hawaii: 187-194.
- Rohlfing T, Brandt R, Menzel R, Maurer CR Jr. 2003. Segmentation of Three-Dimensional Images Using Non-Rigid Registration: Methods and Validation with application to Confocal Microscopy. In: Sonka M, Fitzpatrick JM editors. *Medical Imaging: Image Processing*. Volume No. 5032, SPIE Medical Imaging Conference, San Diego.
- Withers GS, Fahrbach SE, Robinson GE. 1993. Selective neuroanatomical plasticity and division of labour in the honeybee (*Apis mellifera*). *Nature* 364: 238-240.